

ON THE FORMATION OF GLYCOLALDEHYDE (HCOCH₂OH) AND METHYL FORMATE (HCOOCH₃) IN INTERSTELLAR ICE ANALOGS

CHRIS J. BENNETT AND RALF I. KAISER

Department of Chemistry, University of Hawaii at Manoa, Honolulu, HI 96822; kaiser@gold.chem.hawaii.edu

Received 2006 December 18; accepted 2007 February 12

ABSTRACT

Binary mixtures of methanol (CH₃OH) and carbon monoxide (CO) ices were irradiated at 10 K with energetic electrons to mimic the energy transfer processes that occur in the track of the trajectories of MeV cosmic-ray particles. The formation of glycolaldehyde (HCOCH₂OH) was established through the appearance of new bands in the infrared spectrum at 1757, 1700, 1690, 1367, 1267, and 1067 cm⁻¹. A second C₂H₄O₂ isomer, methyl formate (HCOOCH₃), was also identified by absorptions appearing at 1718, 1159, and 914 cm⁻¹. Mass spectrometer signals during the warm-up of the ice sample showed sublimation of both the glycolaldehyde and methyl formate; these species were monitored via the C₂H₄O₂⁺ molecular ion at mass-to-charge ratio, *m/e*, of 60 originating from both glycolaldehyde and the methyl formate isomer. The latter was distinguishable by the presence of a second signal at *m/e* = 45, i.e., the HCO₂⁺ ion. Kinetic fits of the column densities of the reactants and products suggest the initial step of the formation process is the cleavage of a C–H bond in the methanol molecule to generate either the hydroxymethyl (CH₂OH) or methoxy (CH₃O) radical plus atomic hydrogen. The hydrogen atom holds excess kinetic energy, allowing it to overcome entrance barriers required; therefore, a hydrogen could add to a CO molecule, generating the formyl radical (HCO). This can recombine with the hydroxymethyl radical to form glycolaldehyde or with the methoxy radical to yield methyl formate. Similar processes are expected to form glycolaldehyde and methyl formate in the interstellar medium on grains and possibly on cometary ices, thus providing alternatives to gas-phase processes for the generation of complex species whose fractional abundances compared with H₂ of typically a few times 10⁻⁹ cannot be accounted for solely by gas-phase chemistry.

Subject headings: cosmic rays — ISM: molecules — methods: laboratory — molecular processes — planets and satellites: general

Online material: color figures

1. INTRODUCTION

The majority of interstellar gas-phase molecules that have been detected are found in regions of space known as hot molecular cores. These locations typically have high temperatures ($T > 150$ K) and high number densities ($n > 10^6$ cm⁻³) and are thought to be the birthplace of high-mass stars (Linz et al. 2005; Kurtz 2006). Of the 135 molecular species detected to date, more than half have been discovered in the hot core known as the Large Molecule *Heimat*, located in Sagittarius B2(N) [Sgr B2(N)–LMH; Snyder 2006]. Of the chemical species detected so far, special attention has been paid to the formation of different isomers such as C₂H₄O (acetaldehyde, ethylene oxide, vinyl alcohol) and C₂H₄O₂ (glycolaldehyde, methyl formate, acetic acid), that is, molecules that have the same chemical formula but differ in the way atoms are connected. Here the elucidation of their formation mechanisms can provide insight into the present and past physicochemical conditions of the clouds and molecular cores (Hollis et al. 2000). In this paper, we choose to investigate the formation routes of the C₂H₄O₂ isomers detected so far (Fig. 1) because they are of significant astrobiological importance (Remijan et al. 2004; Snyder 2006).

Glycolaldehyde (HCOCH₂OH) is a hydroxyaldehyde diose and represents the simplest member of the monosaccharide sugars. It could be involved in the production of important biomolecules such as glycolaldehyde phosphates, amino acids, and more complex carbohydrates including ribose (also a monosaccharide), which serves as part of the structural backbone of ribonucleic acid (Collins & Ferrier 1995; Weber 1998; Krishnamurthy et al. 1999). The production of sugars from formaldehyde through the

formose reaction (Boutlerow 1861) in a primitive Earth environment is unlikely, because of the harsh conditions involved (strongly alkaline, moderate temperature, high formaldehyde concentrations, catalytic). Indeed, the primordial production of sugars via the formose reaction has been seriously questioned by Shapiro (1988). Hollis et al. (2000) detected the presence of glycolaldehyde within Sgr B2(N)–LMH, and although this is the only source where it has been identified, several subsequent studies have confirmed its presence (Hollis et al. 2001, 2004; Halfen et al. 2006). In a recent attempt to confine the abundances of complex species present in comet C/1995 O1 (Hale-Bopp), Despois et al. (2005) presented an upper limit for the abundance of glycolaldehyde relative to water of 0.04. This could have profound implications from an astrobiological viewpoint, considering that comets are thought to preserve the “pristine” interstellar material from which our solar system was formed and are also considered as a source for prebiotic molecules to seed Earth (Chyba & Sagan 1992; Ehrenfreund et al. 2004; Tornow et al. 2005).

Acetic acid (CH₃COOH) is also considered to be a molecule of astrobiological importance, acting as a precursor to the amino acid glycine (see, e.g., Sorrell 2001). Acetic acid was first detected in the hot molecular core Sgr B2(N)–LMH by Mehringer et al. (1997). Since then it has also been observed in several other hot molecular cores (Remijan et al. 2002, 2003), in high-mass star-forming regions (Remijan et al. 2004), in the low-mass protostar IRAS 16293–2422 (Cazaux et al. 2003), and also toward the proto-planetary nebula CRL 618 (Remijan et al. 2005). It has also been found within the Murchison meteorite; upper limits of 0.06 relative to water were also suggested in comet Hale-Bopp (Huang et al. 2005; Despois et al. 2005).

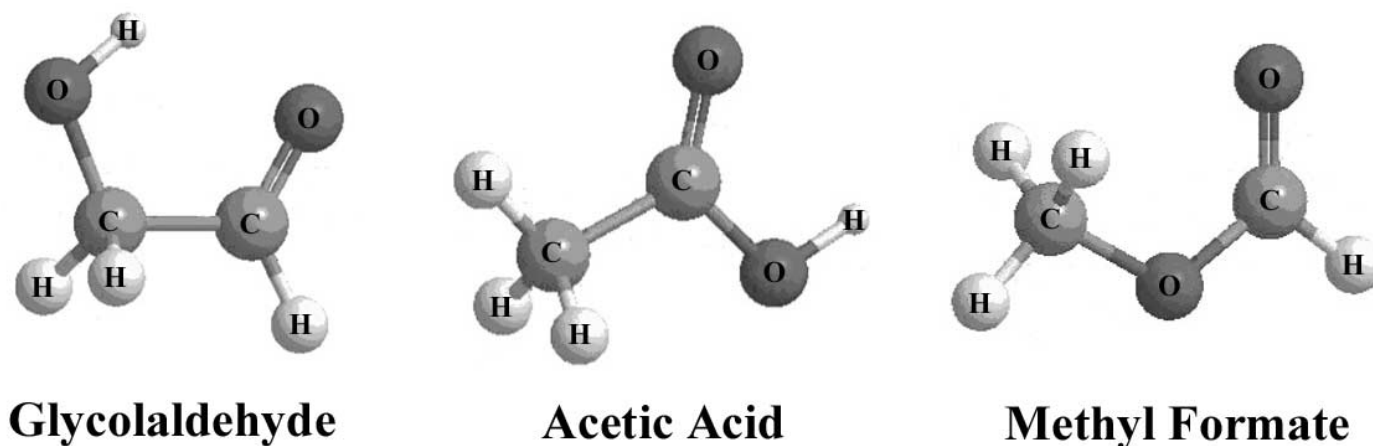


FIG. 1.—Three different C₂H₄O₂ isomers that have been observed in the interstellar medium. [See the electronic edition of the Journal for a color version of this figure.]

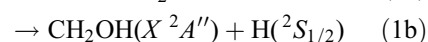
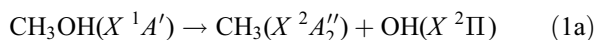
Methyl formate (HCOOCH₃) was first detected in the hot molecular core Sgr B2(N) by Brown et al. (1975), but it has also been monitored in Orion A (Eldér et al. 1980), G34+0.15 (Macdonald et al. 1996), G327.3–0.6 (Gibb et al. 2000), and the low-mass star-forming region IRAS 16293–2422 (Remijan & Hollis 2006) and also toward the proto-planetary nebula CRL 618 (Remijan et al. 2005). Besides comet Hale-Bopp, where its abundance has been estimated as 0.08 relative to water, methyl formate has also been found in comet C/2002 T7 (LINEAR), for which an upper limit of 0.01 relative to water was presented (Despois et al. 2005; Remijan et al. 2006).

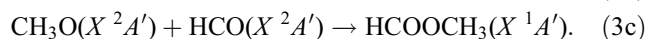
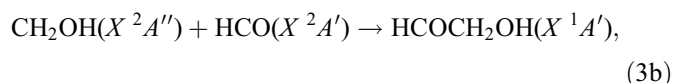
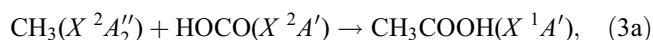
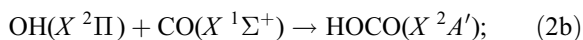
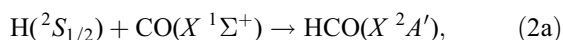
As already stated, Sgr B2(N)–LMH represents the only source where all three of these isomers have been detected. Hollis et al. (2001) reported the relative abundances of these three isomers as being 52:2:1 (methyl formate:acetic acid:glycolaldehyde). However, using the most recently determined column density for glycolaldehyde of 5.9×10^{13} molecules cm⁻² (Halfen et al. 2006) and values of 6.1×10^{15} molecules cm⁻² for acetic acid (Remijan et al. 2002) and 1.1×10^{17} molecules cm⁻² for methyl formate (Liu et al. 2001), updated relative abundances of these isomers have been reported to be 1864:103:1. Taking the column density of H₂ as 3×10^{24} molecules cm⁻² (Nummelin et al. 2000), this gives fractional abundances (relative to H₂) of 2.0×10^{-11} , 2.0×10^{-9} , and 3.7×10^{-8} for glycolaldehyde, acetic acid, and methyl formate, respectively. However, while both methyl formate and acetic acid are confined to a compact source around 5'' in diameter, glycolaldehyde is extended as far as $\geq 60''$ (Hollis et al. 2001). It has been suggested that the extended distribution of glycolaldehyde may be the result of chemistry initiated by the heating of interstellar grains by shocks (Chengalur & Kanekar 2003).

Chemical models that attempt to reproduce the column densities of these isomers based solely on gas-phase pathways have failed by orders of magnitude. To our knowledge, no models currently exist that attempt to reproduce the column density specifically of glycolaldehyde. However, regarding acetic acid, gas-phase models of Sgr B2(N) predict fractional abundances of only 2×10^{-11} and 3×10^{-12} molecules cm⁻² (Wlodarczyk & Demaison 1988; Wootten et al. 1992). The formation of methyl formate by gas-phase synthesis alone similarly falls short by an order of magnitude (Horn et al. 2004). More recent modeling has been attempted to reproduce the column densities of these isomers, taking into account reactions that occur on the surfaces of interstellar grains. However, even these models are limited,

as they are primarily based on the surface migration of radicals (e.g., Garrod & Herbst 2006) or of heavy atoms (Charnley & Rodgers 2006). It has long been known that surface migration on these icy grains involves overcoming large diffusion barriers, making these processes inefficient for species other than hydrogen. Therefore, it seems unlikely that diffusion-limited processes on grain surfaces can form complex organic molecules (Leitch-Devlin & Williams 1984).

However, it is well known that during the lifetimes of about $(4\text{--}6) \times 10^8$ yr (Jones 2005) of interstellar ices within dense molecular clouds, these ices are subject to irradiation from UV photons, as well as Galactic cosmic rays (GCRs). This ionizing radiation field can chemically modify the pristine ices as condensed on interstellar grains. The UV photons typically have energies less than 13.6 eV and a fluence of $\phi = 10^3$ photons cm⁻² s⁻¹ (Prasad & Tarafdar 1983); they only penetrate the outer mono layers of the ice-coated interstellar grains. The GCRs consist of about 98% protons (*p*, H⁺) and 2% helium nuclei (α -particles, He⁺²) and have a distribution maximum around 1 MeV with $\phi = 10$ particles cm⁻² s⁻¹ (Strazzulla & Johnson 1991). Detailed collisional cascade calculations demonstrate that each MeV cosmic-ray particle can penetrate the entire icy grain and induce cascades, generating up to 10^2 suprathreshold particles (Kaiser et al. 1997; Kaiser 2002). The energy transferred to the ices is sufficient to ionize the molecules and hence generate high-energy electrons, which may be born with kinetic energies up to a few keV. It has been shown that for a 10 MeV proton, 99.99% of the energy transferred into the ice target will be to the electronic system of the target molecules by means of a linear energy transfer (LET) of a few keV per micron; a similar LET is found for 5 keV electrons as they penetrate ices (for more detailed discussions on the effects of irradiation on ices, see Johnson 1990; Spinks & Woods 1990; Kaiser et al. 1997; Kaiser 2002; Bennett et al. 2005). Therefore, to study the formation of C₂H₄O₂ isomers within interstellar ices, we chose to investigate the effects of 5 keV electrons on binary ice mixtures of carbon monoxide and methanol, both of which are found to be abundant within interstellar ices (e.g., Gibb et al. 2004). Here the radiolysis-induced production of C₂H₄O₂ isomers could occur via the following reactions:





First, methanol undergoes a unimolecular decomposition to produce either the methyl and hydroxyl radicals (1a), the hydroxymethyl radical and a hydrogen atom (1b), or the methoxy radical and a hydrogen atom (1c). Second, one of the radicals produced can add to carbon monoxide to produce either the formyl radical (2a) or the carboxyl radical (2b). Finally, these radicals can recombine to produce acetic acid (3a), glycolaldehyde (3b), or methyl formate (3c). In this paper, we simulate the effects of ionizing radiation on ice-analog samples in the interstellar medium and on comets and investigate how distinct C₂H₄O₂ isomers are formed in binary ice mixtures of carbon monoxide and methanol.

2. EXPERIMENTAL

The experiments were carried out in a stainless steel ultra-high-vacuum chamber, where pressures as low as 3×10^{-11} torr can be achieved through the use of oil-free magnetically suspended turbomolecular pumps. The gas mixture was prepared in a separate chamber from 20 mbar of methanol (Fisher Chemicals 99.9%, further purified by a foreline nitrogen cold trap) and 40 mbar of carbon monoxide (Specialty Gas Group 99.99%). The gas mixture is deposited onto a highly polished silver (111) monocrystal target held at 11.1 ± 0.3 K through a glass capillary array held 5 mm from the silver target. The gas is allowed to condense for 50 minutes; during this process, the background pressure in the main chamber is kept constant at 10^{-8} torr. The silver target (which is freely rotatable) is then moved into position so that the freshly condensed ice can be monitored by a Nicolet 510 DX Fourier transform infrared spectrometer, operated in an absorption-reflection-absorption mode (reflection angle $\alpha = 75^\circ$) during irradiation of the sample by the electron gun (Specs EQ 22/35). A quadrupole mass spectrometer (Balzers QMG 420) operating in residual gas analyzer mode with the electron-impact ionization energy at 90 eV allows us to detect any species in the gas phase during the experiment (for more details, see Bennett et al. 2004).

Figures 2a and 2b show the infrared spectrum of the pristine ice sample before the irradiation, held at 11 K; a compilation of the observed bands is listed in Table 1. Note that several new features are observed that are not present in either the pure carbon monoxide ices (Jamieson et al. 2006 and references therein) or pure methanol ices (Bennett et al. 2007 and references therein). These features have been assigned to the formation of a CH₃OH ··· CO complex. To calculate the column densities within our sample, a modified Lambert-Beers relationship is used (Bennett et al. 2004). The column density of carbon monoxide was derived from the ¹³CO ν_1 fundamental band at 2090 cm⁻¹, using an absorption coefficient of 1.5×10^{-19} cm molecule⁻¹ of ¹²CO (Gerakines et al. 2005). The derived column density was found to be $(5.24 \pm 0.30) \times 10^{17}$ molecules cm⁻². For methanol, the column density was derived from the ν_8 fundamental band at 1030 cm⁻¹ using an *A*-value of 1.3×10^{-17} cm molecule⁻¹ (Palumbo et al. 1999). Here the column density was found to be

$(3.36 \pm 0.22) \times 10^{17}$ molecules cm⁻², indicating that the ratio of methanol to carbon monoxide within our ice sample is approximately 1:1.5. If we assume that the densities of carbon monoxide and methanol are 1.029 and 1.020 g cm⁻³, respectively, we can determine a total ice thickness of 412 ± 18 nm (Jiang et al. 1975; Tauer & Lipscomb 1952).

The ice samples were kept isothermally at 11.1 ± 0.3 K while they were subjected to irradiation from the electron gun at beam currents of 100 nA for 1 hr, scanning the electron beam over an area of 3.0 ± 0.4 cm². This exposes our sample to a total of 2.2×10^{15} electrons (7.5×10^{14} electrons cm⁻²); however, our electron gun has an extraction efficiency of 78.8%, which means the actual number of electrons expected to hit the sample is reduced to 1.8×10^{15} electrons (5.9×10^{14} electrons cm⁻²). Once the irradiation was complete, the sample was left isothermally for an hour, enabling us to establish the stability and/or mobility of species formed. Afterward, a temperature program was started during which the ice was heated at a rate of 0.5 K minute⁻¹ until it reached 300 K. Note that all numerical quantifications listed in this paper are the results of our experiments carried out at 100 nA. Experiments with a lower beam current of 20 nA were also carried out to acquire supplemental mass spectrometry data.

3. RESULTS

3.1. Infrared Band Assignment

Table 2 summarizes the peak positions of the products identified after the condensed ice was subjected to irradiation from 5 keV electrons at 100 nA for 1 hr. Also listed are the products identified previously in irradiation experiments. The approach used here begins with a comparison of the species identified in the irradiation of pure carbon monoxide ices (Jamieson et al. 2006), and then species found in the irradiation of pure methanol ices (Bennett et al. 2007), before presenting any new species uncommon to the irradiation of the pure ices. First, regarding the species also detected in pure carbon monoxide ices, only one novel molecule could be sampled, that is, carbon dioxide, CO₂(X¹Σ_g⁺), where the ν_3 (asymmetric stretch) could be identified at 2342 cm⁻¹ (Fig. 2a), in accordance with previous assignments to this band from carbon dioxide as an amorphous solid at 10 K at 2342 cm⁻¹ (Falk 1987), as well as in the irradiation of pure carbon monoxide at 2346 cm⁻¹ (Jamieson et al. 2006). Two different isotopomers of carbon dioxide could also be identified from their corresponding isotopic shifts for the ν_3 fundamental, where the ¹³CO₂ isomer was found to absorb at 2280 cm⁻¹ and the OC¹⁸O isomer was found to absorb at 2325 cm⁻¹. Again, these values agree well with literature values, where these absorptions were found at 2281 and 2329 cm⁻¹, respectively (Falk 1987), and with the values from Jamieson et al. (2006), who found them at 2281 and 2330 cm⁻¹. The corresponding absorption from the ν_2 (out-of-plane bending) was also found at 660 cm⁻¹, which again agrees well with previous isolation studies of this molecule, in which it has been found to absorb at 661 cm⁻¹ (Falk 1987) or at 660 cm⁻¹ (Jamieson et al. 2006).

A systematic search was carried out for several of the species found to be produced early on during the irradiation of pure carbon monoxide ices. Dicarbon monoxide, C₂O(X³Σ⁻), has been found to have an intense absorption at 1988 cm⁻¹ corresponding to the ν_1 (CO stretch) of this molecule; however, this absorption was undetectable in the present set of experiments. The strongest absorption from tricarbon monoxide occurs at 2249 cm⁻¹ (ν_1 ; CO stretch), the second strongest at 1913 cm⁻¹ (ν_2 ; CC asymmetric stretch). If carbon suboxide, C₃O₂(X¹Σ_g⁺),

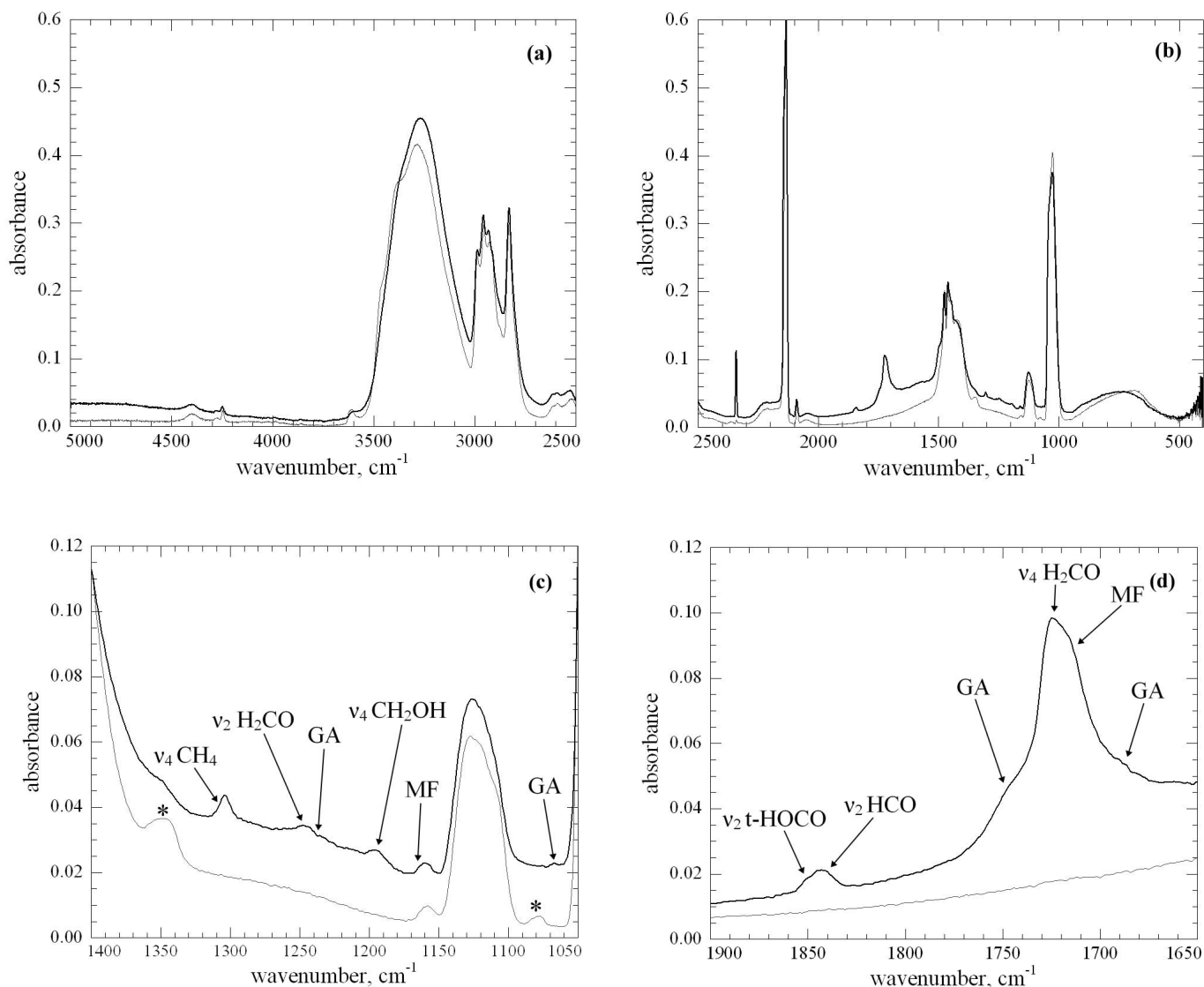


FIG. 2.—Infrared spectra of the CO:CH₃OH frost before irradiation (*gray lines*) and after irradiation with 5 keV electrons at 100 nA for 1 hr (*black lines*): (a) from 2500 to 5000 cm⁻¹; (b) from 400 to 2500 cm⁻¹; (c) between 1050 and 1400 cm⁻¹; (d) between 1650 and 1900 cm⁻¹. Asterisks indicate peaks tentatively assigned to a CO ··· CH₃OH complex. MF = methyl formate, GA = glycolaldehyde.

were present, we should have been able to see the strongest absorptions arising from the ν_3 (CO asymmetric stretch) at 2242 cm⁻¹ and the ν_4 (CC asymmetric stretch) at 1563 cm⁻¹ (Jamieson et al. 2006). Although the ν_3 fundamental overlaps with the $2\nu_8$ band from methanol, which absorbs strongly in this region, the ν_4 vibration would be visible if this species were formed.

Concerning the identification of species also detected within pure methanol ices, here we were able to identify the hydroxymethyl radical, CH₂OH(X^2A'), which was identifiable by its ν_4 (CO stretch) absorption at 1197 cm⁻¹ (Fig. 2*b*), again in good agreement with previous matrix isolation studies of this species, where it has been found to absorb at 1183 cm⁻¹ (Jacox 1981). Other experiments on the irradiation of pure methanol by Bennett et al. (2007) and Gerakines et al. (1996) place this absorption at 1192 and 1197 cm⁻¹, respectively. The latter authors also reported a second band at 1352 cm⁻¹ (ν_5 ; CH₂, OH rocking); however, this band could not be identified. Again, we were unable to directly confirm the presence of the methoxy radical, CH₃O(X^2A'), because its strongest absorptions overlap with those of methanol too closely to be detected (Bennett et al. 2007). The identification of

formaldehyde, H₂CO(X^1A_1), was also possible from the appearance of three of its fundamental bands: the ν_2 (CH₂ rocking) at 1247 cm⁻¹, ν_3 (CH₂ scissoring) at 1500 cm⁻¹, and ν_4 (CO stretching + CH₂ scissoring) at 1718 cm⁻¹ (Figs. 2*c* and 2*d*). These absorptions are found to be in good agreement with formaldehyde within a nitrogen matrix at 11 K, where they appear at 1245, 1499, and 1740 cm⁻¹ (Nelander 1980), as well as with irradiation experiments on pure methanol, where they show up at 1244, 1497, and 1719 cm⁻¹, respectively (Gerakines et al. 1996). The formyl radical, HCO(X^2A'), was identified through the appearance of its ν_2 (CO stretching) fundamental band at 1843 cm⁻¹ (Fig. 2*d*). This value agrees with previous matrix isolation experiments of this radical produced in carbon monoxide matrices, in which it was found to absorb at 1860 cm⁻¹ (Ewing et al. 1960). It also correlates nicely with values from the irradiation of pure methanol, where it was found to absorb at 1842 cm⁻¹ (Bennett et al. 2007). Finally, methane, CH₄(X^1A_1), was found by virtue of an absorption at 1304 cm⁻¹ arising from its ν_4 (deformation) fundamental. This value agrees well with that of methane in an argon matrix, where it is found to absorb at 1304 cm⁻¹ (Fig. 2*c*), as well as with values listed from the irradiation of

TABLE 1
 INFRARED ABSORPTIONS OF THE METHANOL AND CARBON MONOXIDE FROST PRIOR TO IRRADIATION,
 ALONG WITH THE ASSIGNMENTS OF THE OBSERVED BANDS

Band Position (cm ⁻¹)	Assignment	Characterization
4399.....	$\nu_2/\nu_9 + \nu_4/\nu_6/\nu_{10}$ CH ₃ OH	Combination
4275.....	$\nu_2/\nu_9 + \nu_7$ CH ₃ OH?	Combination
4247.....	$2\nu_1$ CO	Overtone
3985.....	CH ₃ OH?	Combination?
3859.....	CH ₃ OH?	Combination?
3610.....	ν_1 CH ₃ OH (CO ... CH ₃ OH)?	Fundamental
3470, 3407, 3288, 3099, 3025.....	ν_1 CH ₃ OH	Fundamental
2988.....	ν_2 CH ₃ OH	Fundamental
2859.....	ν_9 CH ₃ OH	Combination
2925.....	$\nu_4 + \nu_5/\nu_4 + \nu_{10}/\nu_5 + \nu_{10}/2\nu_4/2\nu_{10}/2\nu_5$ CH ₃ OH	Combination/overtone
2871.....	$2\nu_5/2\nu_{10}$ CH ₃ OH	Overtone
2830.....	ν_3 CH ₃ OH	Fundamental
2821.....	$\nu_3/2\nu_6$ CH ₃ OH	Fundamental/overtone
2613, 2588.....	$\nu_4 + \nu_{11}/\nu_7 + \nu_4/\nu_6/\nu_{10}$ CH ₃ OH	Combination
2557, 2516.....	$\nu_6 + \nu_{11}$ CH ₃ OH	Combination
2449.....	$\nu_6 + \nu_8$ CH ₃ OH	Combination
2201.....	$\nu_1 + \nu_L$ CO	Fundamental
2143, 2138, 2132.....	ν_1 CO	Fundamental
2111.....	ν_1 CO-Ag	Fundamental
2089.....	ν_1 ¹³ CO	Isotope peak
2049.....	$2\nu_8$ CH ₃ OH	Overtone
1507.....	$\nu_8 + \nu_{12}$ CH ₃ OH?	Combination
1481, 1478, 1475.....	ν_4 CH ₃ OH	Fundamental
1463, 1457 br.....	ν_{10} CH ₃ OH	Fundamental
1452.....	ν_5 CH ₃ OH	Fundamental
1424.....	ν_6 CH ₃ OH	Fundamental
1405.....	$\nu_{11} + \nu_{12}$ CH ₃ OH?	Combination
1348.....	$\nu_{11} + \nu_{12}$ CH ₃ OH (CO ... CH ₃ OH)?	Fundamental
1158, 1132, 1119, 1106.....	ν_7 CH ₃ OH	Fundamental
1079.....	ν_7 CH ₃ OH (CO ... CH ₃ OH)?	Fundamental
1048, 1045, 1040, 1028.....	ν_8 CH ₃ OH	Fundamental
1013.....	ν_8 ¹³ CH ₃ OH	Isotope peak
887, 831, 719, 664, 597.....	ν_{12} CH ₃ OH	Fundamental

NOTE.—The assignments were aided by characterizations of the pure ices (Jamieson et al. 2006 for carbon monoxide; Bennett et al. 2007 for methanol).

pure methanol, where this band was found to absorb at 1303 cm⁻¹ (Govender & Ford 2000; Bennett et al. 2007)

Considering the new species formed in the binary mixture, methyl formate, HCOOCH₃(*X*¹*A'*), was identifiable through its ν_{14} (CO of CHO stretching) fundamental band at 1718 cm⁻¹, its ν_8 (COC asymmetric stretch) band at 1159 cm⁻¹, and its ν_5 (CO of OCH₃ stretching) band at 914 cm⁻¹ (Figs. 2*c* and 2*d*). These values agree well with those of the *cis* (*syn*) form of methyl formate, where the same absorptions are found to absorb at 1708, 1158, and 922 cm⁻¹ in an argon matrix (Blom & Günthard 1981). The *trans* (*anti*) conformer has a strong absorption at 1099 cm⁻¹ from the ν_9 fundamental (Müller et al. 1983), which was unidentifiable in the current experiments. Glycolaldehyde, HCOCH₂OH(*X*¹*A'*), found as its lowest conformer, commonly referred to as Cc (*cis-cis* bonding within the OCCO backbone, as shown in Fig. 1), was identified by its ν_{14} (CO stretch) fundamental at 1757 cm⁻¹, as observed previously in pure methanol ices (Fig. 2*d*; Bennett et al. 2007). This band is actually one of two expected as a result of Fermi resonance splitting of the ν_{14} (CO stretch) fundamental and an overtone from the $2\nu_6$ (CC stretch) band, whereby this second band was found to occur around 1700 and 1690 cm⁻¹ (Fig. 2*c*; Jetzki et al. 2004). We were also able to find absorptions from the ν_{11} (CH of CHO rocking) fundamental at 1367 cm⁻¹ and the

ν_9 (OH rocking and CH₂ wagging) fundamental at 1267 cm⁻¹ (Fig. 2*b*). These values are all in good agreement with the Cc conformer of glycolaldehyde within an argon matrix at 13 K, where these absorptions can be found at 1747, 1700, 1367, and 1267 cm⁻¹, respectively (Aspiala et al. 1986). Note that an additional peak at 1067 cm⁻¹ was found, which has been assigned to the ν_7 (CO stretch) from the Tt (*trans-trans*) conformer of glycolaldehyde located at 1065 cm⁻¹ within an argon matrix (Fig. 2*c*; Aspiala et al. 1986).

As with the pure methanol system, several molecules that were searched for could not be identified within the current experiments. These include the hydroxyl radical, OH(*X*²II), the fundamental absorption of which may overlap with methanol, which has been experimentally determined in matrix-isolated experiments to absorb at 3548 cm⁻¹ (Cheng et al. 1988). The methyl radical, CH₃(*X*²*A'*), which is seen most easily by its ν_1 (CH₃ wagging) fundamental, which absorbs in, for example, nitrogen matrices at 611 cm⁻¹ (Milligan & Jacox 1967), also could not be unambiguously identified in these experiments. However, the carboxyl radical, HOCO(*X*²*A'*), was detected through its ν_2 (CO stretching) absorption at 1852 cm⁻¹ (Fig. 2*d*); this is consistent with the *trans* isomer, which has previously been identified at 1846 cm⁻¹ in an argon matrix (Jacox 1988) and at 1833 cm⁻¹ in a carbon monoxide matrix (Milligan & Jacox 1971).

TABLE 2
OBSERVED PEAK POSITIONS, ASSIGNMENTS, AND CHARACTERIZATIONS AFTER 1 HOUR
OF IRRADIATION WITH 5 keV ELECTRONS AT 100 nA

Band Position (cm ⁻¹)	Literature Position (cm ⁻¹)	Assignment	Characterization
Bands Common to Irradiation of Pure Carbon Monoxide ^a			
3700.....	3707	$\nu_1 + \nu_3$ CO ₂	Combination
2342.....	2346	ν_3 CO ₂	Fundamental
2325.....	2330	ν_3 OC ¹⁸ O	Isotope peak
2280.....	2281	ν_3 ¹³ CO ₂	Isotope peak
660.....	660	ν_2 CO ₂	Fundamental
Bands Common to Irradiation of Pure Methanol ^b			
1843.....	1841, 1849	ν_3 HCO	Fundamental
1757.....	1747	ν_{14} HCOCH ₂ OH (Cc) Fermi	Fundamental
1726, 1718.....	1718	ν_{14} HCOOCH ₃	Fundamental
	1726	ν_4 H ₂ CO	Fundamental
1500.....	1496	ν_3 H ₂ CO	Fundamental
1304.....	1303	ν_4 CH ₄	Fundamental
1247.....	1245	ν_2 H ₂ CO	Fundamental
1197.....	1192	ν_4 CH ₂ OH	Fundamental
1159.....	1160	ν_8 HCOOCH ₃	Fundamental
1090.....	1090	ν_2 HCO?	Fundamental
		Alcohols	Fundamental
914 br.....	916	ν_5 HCOOCH ₃	Fundamental
Bands Unique to This Experiment			
1852.....	1846 ^c	ν_2 <i>t</i> -HOCO	Fundamental
1700, 1690.....	1700, 1690 ^d	$2\nu_6$ HCOCH ₂ OH Fermi (Cc)	Fundamental
1067.....	1065 ^d	ν_7 HCOCH ₂ OH (Tt)	Fundamental

NOTE.—The band positions of the identified species are compared with our previous studies as well as those found in the literature.

^a Literature values taken from Jamieson et al. (2006) and references therein.

^b Literature values taken from Bennett et al. (2007a) and references therein.

^c Forney et al. (2003).

^d Mohaček-Grošev (2005).

3.2. Mass Spectrometry

The only signal observed through mass spectrometric analysis of the gas phase during irradiation of the sample was found at $m/e = 2$, that is, molecular hydrogen, which immediately ceased when irradiation was stopped, similar to experiments carried out on the irradiation of binary mixtures of methane and carbon monoxide (Bennett et al. 2005). As the sample is warmed up, the carbon monoxide begins to sublime at around 50 K, and methanol around 115 K (Fig. 3). Signal at $m/e = 30$ corresponds to the CH₂O⁺ fragment produced during the dissociative ionization of methanol. From 140 to 180 K, an increase in the signal is observed at $m/e = 60$, corresponding to the C₂H₄O₂⁺ ion; from 155 to 180 K, signal from $m/e = 45$ (HCO₂⁺ fragment) is also observed (Fig. 3). Considering the two different C₂H₄O₂ isomers observed with infrared spectroscopy, it appears that glycolaldehyde, which should have no signal corresponding to an HCO₂⁺ fragment, sublimates between 140 and 160 K, whereas the methyl formate, which should give signal from the HCO₂⁺ fragment, sublimates from 155 to 180 K. The methyl formate appears to be the last molecule to be released from the silver target, as no signal is observed after 180 K. We should mention that it is not possible to distinguish, through mass spectrometry, products produced during the irradiation period from those that may be formed via thermally induced mechanisms (including additional formation of molecules by recombination of previously formed radicals that become mobile during the heating

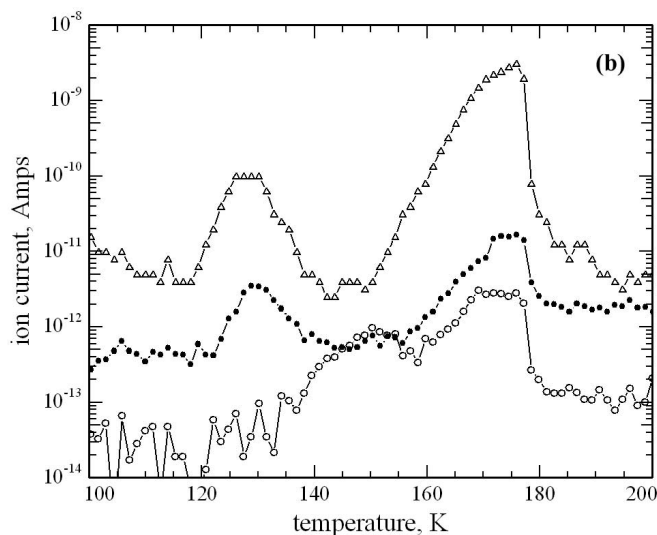


Fig. 3.—Signal from the mass spectrometer, during warm-up of the sample, from $m/e = 30$ (triangles), corresponding to the CH₂O⁺ fragment primarily due to methanol, from $m/e = 45$ (filled circles), corresponding to the CO₂H⁺ fragment, and from $m/e = 60$ (open circles), corresponding to the C₂H₄O₂⁺ ion.

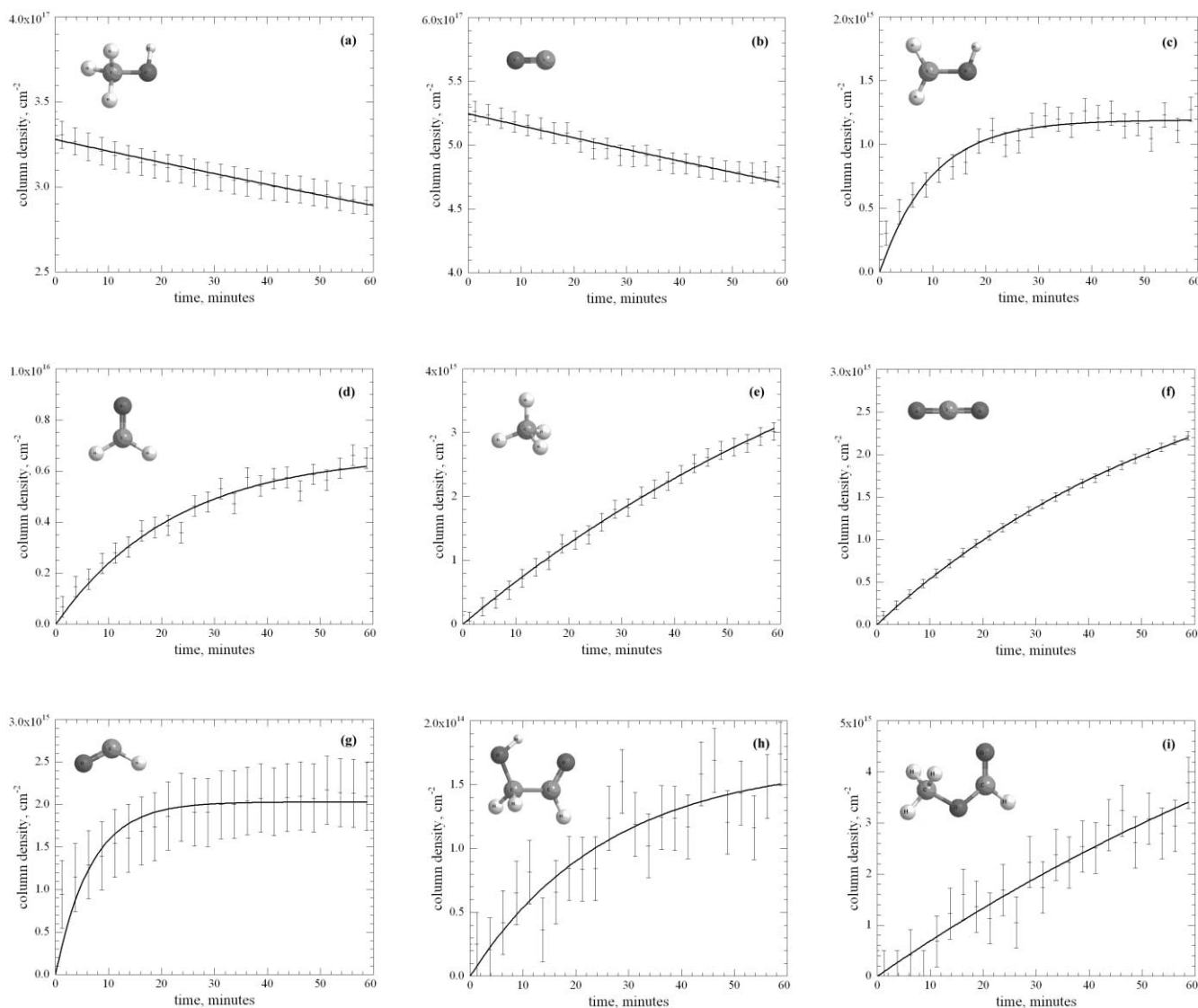
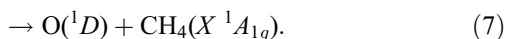
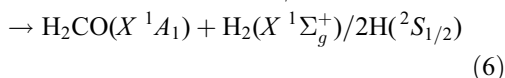
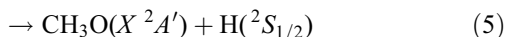
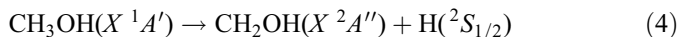


FIG. 4.—Temporal evolution of the new species formed during irradiation along with the lines of best fit from their associated kinetic equations: (a) methanol, (b) carbon monoxide, (c) hydroxymethyl, (d) formaldehyde, (e) methane, (f) carbon dioxide, (g) formyl, (h) glycolaldehyde, (i) methyl formate.

process). However, blank experiments in which samples were not subjected to irradiation failed to give any signals reported here in the mass spectrometer other than at $m/e = 30$, corresponding to the CH_2O^+ fragment from methanol.

4. DISCUSSION

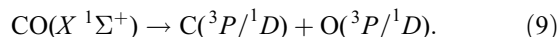
We would now like to discuss the likely formation mechanisms of the observed molecular species in this experiment. Here it is prudent to first discuss the mechanisms observed in the pure ice mixtures. During the irradiation of pure methanol (Bennett et al. 2007), the following primary degradation pathways were indicated:



If the radiolysis-induced decomposition of methanol via reactions (4)–(7) is responsible for the destruction of the methanol molecule, its column density through time should follow first-order kinetic decay as follows:

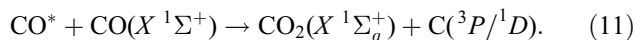
$$[\text{CH}_3\text{OH}]_t = [\text{CH}_3\text{OH}]_0 e^{-k_1 t}. \quad (8)$$

Here the temporal profile of the column density for methanol was produced using the ν_8 fundamental at 1030 cm^{-1} (Palumbo et al. 1999). By fitting our data to equation (8), we determined $[\text{CH}_3\text{OH}]_0 = (3.28 \pm 0.01) \times 10^{17} \text{ molecules cm}^{-2}$ and $k_1 = (3.50 \pm 0.15) \times 10^{-5} \text{ s}^{-1}$ (Fig. 4a). Considering the recent study of irradiation of pure carbon monoxide ices irradiated by 5 keV electrons by Jamieson et al. (2006), they found no evidence for the production of oxygen atoms through the electron-induced decomposition of carbon monoxide,

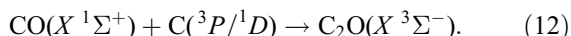


Instead, their results indicated that the decomposition of the carbon monoxide initially involved the excitation of one carbon

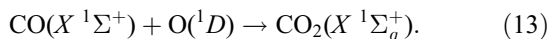
monoxide molecule, followed by a subsequent reaction with a neighboring carbon monoxide molecule to yield carbon dioxide and a free carbon atom:



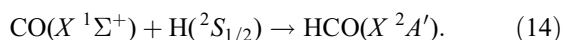
Jamieson et al. suggested that free carbon atoms then react to produce a series of C_nO species via the following reaction sequence:



However, in the present binary mixture, dicarbon oxide was not observed. This can lead us to two conclusions: (1) the carbon atoms produced in reaction (11) react instantly with methanol, and (2) in the case of the binary ice mixture, we do not have sufficient neighboring carbon monoxide molecules for reactions (10) and (11) to proceed. Further, it is feasible for carbon monoxide to be primarily destroyed by reaction with an electronically excited oxygen atom released via reaction (7). Here, if the reaction proceeds on the singlet surface, there is no barrier to the reaction, as compared with reactions of ground-state oxygen with carbon monoxide, which must proceed on the triplet surface and have an associated barrier on the order of 25 kJ mol^{-1} (0.26 eV) calculated from ab initio calculations at the CCSD(T)/Full level of theory (Talbi et al. 2006):



As a second example of a pathway for the destruction of carbon monoxide via reaction with another primary product from the radiolysis-induced decomposition of methanol, we consider the formation of the formyl radical through reaction of carbon monoxide with hydrogen atoms produced in reactions (4)–(6):



The hydrogen atoms produced in reactions (4)–(6) will likely be born with excess kinetic energy, allowing them to overcome the barrier for addition of carbon monoxide of 11 kJ mol^{-1} (0.12 eV) as calculated by Bennett et al. (2005) using the CCSD(T)/aug-cc-pVTZ level of theory. Whether the carbon monoxide molecule is decomposed through radiolysis by the impinging electrons or through reactions with the products of the radiolysis of methanol, its temporal profile should still be fitted by first-order kinetics as with methanol (or pseudo-first-order, in the case of reactions with products from the decomposition of methanol). Here we were able to fit the temporal profile of carbon monoxide to the following equation:

$$[\text{CO}]_t = [\text{CO}]_0 e^{-k_2 t}. \quad (15)$$

Using an A -value of $1.5 \times 10^{-19} \text{ cm molecule}^{-1}$ for the ^{13}C isotope peak of the carbon monoxide ν_1 fundamental appearing at 2090 cm^{-1} , fitting our data to equation (15) yielded $[\text{CO}]_0 = (5.25 \pm 0.01) \times 10^{17} \text{ molecules cm}^{-2}$ and $k_2 = (3.05 \pm 0.12) \times 10^{-5} \text{ s}^{-1}$ (Fig. 4b).

From the discussions above, it follows that the production of the primary degradation products of methanol produced through reactions (4)–(7) should also follow first-order kinetics, giving

$$[\text{CH}_2\text{OH}] = a(1 - e^{-k_3 t}), \quad (16)$$

$$[\text{CH}_3\text{O}] = b(1 - e^{-k_4 t}), \quad (17)$$

$$[\text{H}_2\text{CO}] = c(1 - e^{-k_5 t}), \quad (18)$$

$$[\text{CH}_4] = d(1 - e^{-k_6 t}). \quad (19)$$

Considering the hydroxymethyl radical, we traced the temporal evolution of its column density using the ν_4 fundamental at 1197 cm^{-1} and an A -value of $1.56 \times 10^{-17} \text{ cm molecule}^{-1}$ (Bennett et al. 2007) and fitted it to equation (16). Here we found $a = (1.19 \pm 0.02) \times 10^{15} \text{ molecules cm}^{-2}$ and $k_3 = (1.69 \pm 0.15) \times 10^{-3} \text{ s}^{-1}$ (Fig. 4c). Unfortunately, as we were unable to spectroscopically observe the methoxy radical, no temporal profile could be produced and hence no fitting could be achieved. However, formaldehyde was followed through its ν_2 fundamental at 1250 cm^{-1} using an A -value of $2.44 \times 10^{-18} \text{ cm molecule}^{-1}$ (Bennett et al. 2007). By fitting our results to equation (18), we found $b = (6.68 \pm 0.25) \times 10^{15} \text{ molecules cm}^{-2}$ and $k_5 = (7.37 \pm 0.67) \times 10^{-4} \text{ s}^{-1}$ (Fig. 4d). For methane, the ν_4 fundamental at 1300 cm^{-1} was used to produce a temporal profile with an A -value of $7.0 \times 10^{-18} \text{ cm molecule}^{-1}$ (Kerkhof et al. 1999). Using equation (19), our results indicate that $d = (6.64 \pm 0.41) \times 10^{15} \text{ molecules cm}^{-2}$ and $k_6 = (1.76 \pm 0.14) \times 10^{-4} \text{ s}^{-1}$ (Fig. 4e).

Considering the formation of carbon dioxide through either reactions involving excited carbon monoxide ([10] and [11]), or the formation of excited oxygen atoms from methanol through reaction (7) followed by addition of the excited oxygen atom to carbon monoxide, reaction (13), the kinetics could be considered as pseudo-first-order if we assume that reactions (10) and (7) will proceed more quickly than reactions (11) and (13), respectively. Here the temporal profile of the column density of carbon dioxide should be fitted via equation (20). For carbon dioxide, an A -value of $7.6 \times 10^{-17} \text{ cm molecule}^{-1}$ (Gerakines et al. 1995) was used for the ν_3 fundamental at 2342 cm^{-1} to produce the temporal profile. After fitting the data to the equation

$$[\text{CO}_2] = e(1 - e^{-k_7 t}), \quad (20)$$

we found $e = 3.56 \pm 0.07 \times 10^{15} \text{ molecules cm}^{-2}$ and $k_7 = (2.72 \pm 0.01) \times 10^{-3} \text{ s}^{-1}$ (Fig. 4f).

Similarly, for the formyl radical, which can be formed through reaction (14), the addition of hydrogen to carbon monoxide, we can expect its generation to follow pseudo-first-order kinetics, where

$$[\text{HCO}] = f(1 - e^{-k_8 t}). \quad (21)$$

By using the ν_2 fundamental at 1843 cm^{-1} with an A -value of $1.48 \times 10^{-17} \text{ cm molecule}^{-1}$ (Bennett et al. 2005), we were able to reproduce the temporal column density of this species and fit the data to equation (21). The results give $f = (2.03 \pm 0.04) \times 10^{15} \text{ molecules cm}^{-2}$ and $k_8 = (2.51 \pm 0.30) \times 10^{-3} \text{ s}^{-1}$ (Fig. 4g).

Now we would like to consider the formation of glycolaldehyde and methyl formate. We propose that the formation of these species occurs by means of the barrierless recombination of neighboring molecules in the correct orientation, formed during

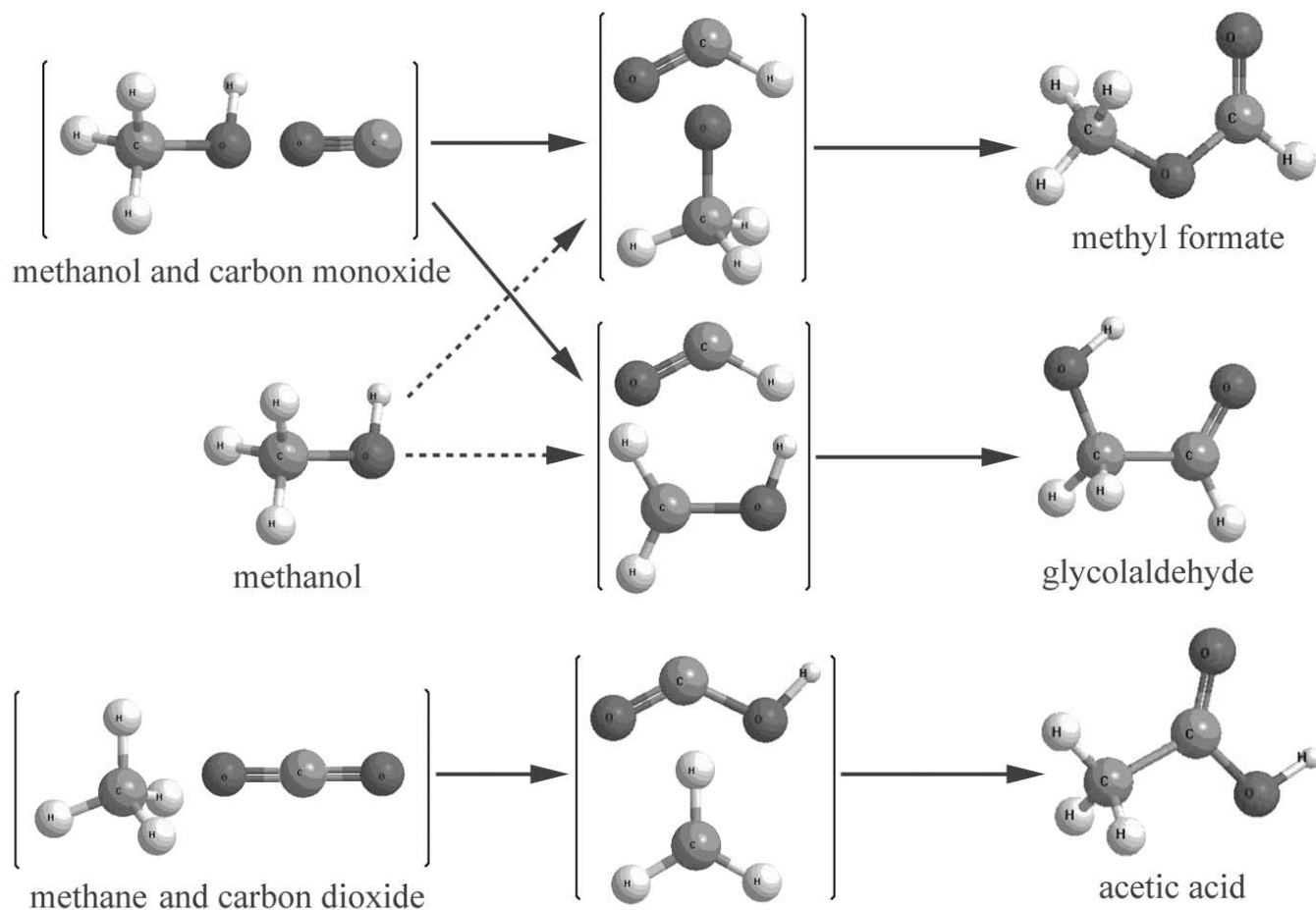


FIG. 5.—Summary of pathways to form C₂H₄O₂ isomers via the three interstellar ice analogs of different compositions investigated so far. Dashed arrows indicate processes where several steps may be required to generate the appropriate radical species (see Bennett et al. 2007 for more details). [See the electronic edition of the *Journal* for a color version of this figure.]

the irradiation process. Here the formation of glycolaldehyde will follow the recombination of a hydroxymethyl and formyl radical:



The formation of methyl formate can occur by means of a similar process involving the methoxy radical instead of the hydroxymethyl radical:



Assuming that once these radicals are formed within the same matrix cage in the correct geometric orientation to recombine, we can again take the production of these species to follow pseudo-first-order kinetics, giving

$$[\text{HCOCH}_2\text{OH}] = g(1 - e^{-k_9 t}), \quad (24)$$

$$[\text{HCOOCH}_3] = h(1 - e^{-k_{10} t}). \quad (25)$$

For glycolaldehyde, we used the ν_7 fundamental of the Tt conformer at 1065 cm⁻¹ with an A -value of 1.04 × 10⁻¹⁷ cm molecule⁻¹ (Bennett et al. 2007) to produce the temporal profile of the column density. Note that no suitable peak from the Cc conformer could be used for the purpose of con-

structing a temporal profile, and thus more glycolaldehyde was produced in our experiments than we are able to quantify. Fitting the data to equation (24) yields results of $g = (1.68 \pm 0.19) \times 10^{14}$ molecules cm⁻² and $k_9 = (6.40 \pm 1.58) \times 10^{-4}$ s⁻¹ (Fig. 4h). Regarding methyl formate, the temporal profile was produced from the evolution of the ν_5 fundamental at 920 cm⁻¹, with an A -value of 4.0 × 10⁻¹⁸ cm molecule⁻¹ (Bennett et al. 2007). Here, fitting the data to equation (25) gives values of $h = (9.51 \pm 6.11) \times 10^{15}$ molecules cm⁻² and $k_{10} = (1.26 \pm 0.958) \times 10^{-4}$ s⁻¹ (Fig. 4i).

Although the products produced during the irradiation of the binary ice mixture studied here are the same as those from the irradiation of pure methanol ices as studied by Bennett et al (2007), a few comments should be made about the similarities and differences of these systems. Because of different ice thicknesses, this discussion will remain qualitative. As carbon monoxide is present in the initial ice mixture here, we produce comparatively higher column densities of several species that may form as a result of reaction with this species, including the formyl radical and carbon dioxide. It is interesting to note the relative production rates of the hydroxymethyl radical versus formaldehyde, where we find that more formaldehyde is produced in the binary ice mixture whereas the hydroxymethyl radical is not as abundant. Presumably, this is a result of the fact that there are more carbon and oxygen atoms in a reduced form within the ice

mixture, where formaldehyde represents an intermediate level of saturation. In both systems, the production of methyl formate is more efficient than that of glycolaldehyde by an order of magnitude. No evidence was found for the production of acetic acid within either system, whereby our proposed formation route involved the cleavage of the C-O sigma bond in methanol to form the methyl and hydroxyl radicals (reaction [1a]). As neither of these radicals could be detected within our system, we conclude that upon irradiation by electrons, methanol does not efficiently decompose by this pathway.

5. ASTROPHYSICAL IMPLICATIONS

Our research indicates that it is likely for both methyl formate and glycolaldehyde to be formed within interstellar ices subjected to irradiation, provided that carbon monoxide and methanol can be found as neighboring molecules. Is there any evidence of this from observations of interstellar ices? Recently, Gibb et al. (2004) carried out a survey of 23 infrared sources using the *Infrared Space Observatory (ISO)*, in which they found the presence of both methanol and carbon monoxide as constituents of the icy grains in 15 of the sources. Typically, the abundances relative to water of carbon monoxide and methanol were found to be around 3%–25% and 3%–15%, respectively. One particular infrared source in the Corona Australis molecular cloud complex known as R CrA IRS 2 was found to have upper limits of 53% and 46% for carbon monoxide and methanol relative to water; however, does this mean that they are likely to reside close enough to react as the ices are subjected to irradiation? Interstellar ices are generally considered to consist of a silicate/carbonaceous core covered by both a polar and an apolar layer in which the majority of the methanol resides in the polar layer, whereas the majority of the carbon monoxide is found in the outer, more volatile apolar ice layer (Allamandola et al. 1999). Taking this into account, it seems likely that only carbon monoxide that has been identified as being present within the polar ice layer is likely to be able to react with methanol in a way similar to our experiments. In the case of R CrA IRS 2, the amount of carbon monoxide thought to exist within the polar matrix is reduced to 2.6% relative to water, whereby the majority of neighboring molecules are likely to be water. However, some of the interstellar ices covered in the study are found to have an abundance of up to 13% of carbon monoxide within the polar ices, which could have methanol molecules as nearest neighbors. A quantitative extrapolation as to how much glycolaldehyde and methyl formate could be produced by irradiation of interstellar ices is difficult at this stage, as the actual ice

morphology is poorly understood. However, our results do agree qualitatively with the abundances reported within the interstellar medium, in that the production of methyl formate was found to be much more efficient than the production of glycolaldehyde. Although the third isomer, acetic acid, was not found to be produced during the irradiation of methanol/carbon monoxide ices, we have shown that it can be produced in mixtures of methane and carbon dioxide (Bennett & Kaiser 2007), and thus solid-state formation mechanisms for all three C₂H₄O₂ isomers by the irradiation of interstellar ices are likely to exist. Figure 5 illustrates pictorially the ice mixtures studied so far that have been found to produce the three C₂H₄O₂ isomers presently detected within the interstellar medium. The abundance of C₂H₄O₂ isomers within interstellar ices is expected to be less than 1% relative to water and therefore likely below the present detection limits of, for example, *ISO*. The main difficulty lies in the fact that the strongest bands from these species (e.g., C=O stretching bands) overlap with those from other species already thought to be present within these ices (such as formaldehyde [5.81 μm], formic acid [5.85 μm], and acetaldehyde [5.83 μm]; Gibb et al. 2004). The best candidate for detection of C₂H₄O₂ isomers within interstellar ices would probably be methyl formate, because of its predicted higher abundance; if a high enough concentration exists, its presence could be confirmed through absorptions from the ν₅ fundamental around 914 cm⁻¹ (10.94 μm), although this would be difficult to distinguish from the strong underlying broad absorption from the silicate core that occurs around 1030 cm⁻¹ (9.70 μm), as well as from other species whose presence is predicted but not confirmed within interstellar ices, such as ethylene, which absorbs at 951 cm⁻¹ (10.52 μm). Once these molecules are formed within these interstellar ices, they can subsequently be released into the gas phase as the icy mantle begins to sublime when a young stellar object begins to form. Thus, it is important for these processes to be included in future models of hot molecular cores to account for the number densities of these species found from astronomical observations.

This material is based upon work supported by the National Aeronautics and Space Administration through the NASA Astrobiology Institute under cooperative agreement NNA04CC08A issued through the Office of Space Science. We are also grateful to Ed Kawamura (University of Hawaii at Manoa, Department of Chemistry) for his support.

REFERENCES

- Allamandola, L. J., Bernstein, M. P., Sandford, S. A., & Walker, R. L. 1999, *Space Sci. Rev.*, 90, 219
 Aspiala, A., Murto, J., & Stén, P. 1986, *Chem. Phys.*, 106, 399
 Bennett, C. J., Chen, S.-H., Sun, B.-J., Chang, A. H. H., & Kaiser, R. I. 2007, *ApJ*, 660, 1588
 Bennett, C. J., Jamieson, C., Mebel, A. M., & Kaiser, R. I. 2004, *Phys. Chem. Chem. Phys.*, 6, 735
 Bennett, C. J., Jamieson, C. S., Osamura, Y., & Kaiser, R. I. 2005, *ApJ*, 624, 1097
 Bennett, C. J., & Kaiser, R. I. 2007, *ApJ*, 660, 1289
 Blom, C. E., & Günthard, H. H. 1981, *Chem. Phys. Lett.*, 84, 267
 Boutlerow, M. A. 1861, *CR Acad. Sci. Paris*, 53, 145
 Brown, R. D., Crofts, J. G., Gardner, F. F., Godfrey, P. D., Robinson, B. J., & Whiteoak, J. B. 1975, *ApJ*, 197, L29
 Cazaux, S., Tielens, A. G. G. M., Ceccarelli, C., Castets, A., Wakelam, V., Caux, E., Parise, B., & Teyssier, D. 2003, *ApJ*, 593, L51
 Charnley, S. B., & Rodgers, S. D. 2006, in *IAU Symp. 231, Astrochemistry: Recent Successes and Current Challenges*, ed. D. C. Lis, G. A. Blake, & E. Herbst (Cambridge: Cambridge Univ. Press), 237
 Cheng, B.-M., Lee, Y.-P., & Ogilvie, J. F. 1988, *Chem. Phys. Lett.*, 151, 109
 Chengalur, J. N., & Kanekar, N. 2003, *A&A*, 403, L43
 Chyba, C., & Sagan, C. 1992, *Nature*, 355, 125
 Collins, P., & Ferrier, R. 1995, *Monosaccharides: Their Chemistry and Their Roles in Natural Products* (Wiley: New York)
 Despois, D., Biver, N., Bockelée-Morvan, D., & Crovisier, J. 2005, in *IAU Symp. 231, Astrochemistry: Recent Successes and Current Challenges*, ed. D. C. Lis, G. A. Blake, & E. Herbst (Cambridge: Cambridge University Press), 469
 Ehrenfreund, P., Charnley, S. B., & Wooden, D. 2004, in *Comets II*, ed. M. C. Festou, H. U. Keller, & H. A. Weaver (Tucson: Univ. Arizona Press), 115
 Eilddér, J., et al. 1980, *ApJ*, 242, L93
 Ewing, G. E., Thompson, W. E., & Pimentel, G. C. 1960, *J. Chem. Phys.*, 32, 927 (erratum 34, 1067 [1961])
 Falk, M. 1987, *J. Chem. Phys.*, 86, 560
 Forney, D., Jacox, M. E., & Thompson, W. E. 2003, *J. Chem. Phys.*, 119, 10814
 Garrod, R. T., & Herbst, E. 2006, *A&A*, 457, 927
 Gerakines, P. A., Bray, J. J., Davis, A., & Richey, C. R. 2005, *ApJ*, 620, 1140
 Gerakines, P. A., Schutte, W. A., & Ehrenfreund, P. 1996, *A&A*, 312, 289
 Gerakines, P. A., Schutte, W. A., Greenberg, J. M., & van Dishoeck, E. F. 1995, *A&A*, 296, 810
 Gibb, E., Nummelin, A., Irvine, W. M., Whittet, D. C. B., & Bergman, P. 2000, *ApJ*, 545, 309

- Gibb, E. L., Whittet, D. C. B., Boogert, A. C. A., & Tielens, A. G. G. M. 2004, *ApJS*, 151, 35
- Govender, M. G., & Ford, T. A. 2000, *J. Mol. Struct.*, 550, 445
- Halfen, D. T., Apponi, A. J., Woolf, N., Polt, R., & Ziurys, L. M. 2006, *ApJ*, 639, 237
- Hollis, J. M., Jewell, P. R., Lovas, F. J., & Remijan, A. 2004, *ApJ*, 613, L45
- Hollis, J. M., Lovas, F. J., & Jewell, P. R. 2000, *ApJ*, 540, L107
- Hollis, J. M., Vogel, S. N., Snyder, L. E., Jewell, P. R., & Lovas, F. J. 2001, *ApJ*, 554, L81
- Horn, A., Møllendal, H., Sekiguchi, O., Uggerud, E., Roberts, H., Herbst, E., Viggiano, A. A., & Fridgen, T. D. 2004, *ApJ*, 611, 605
- Huang, Y., Wang, Y., Alexandre, M. R., Lee, T., Rose-Petrucci, C., Fuller, M., & Pizzarello, S. 2005, *Geochim. Cosmochim. Acta*, 69, 1073
- Jacox, M. E. 1981, *Chem. Phys.*, 59, 213
- . 1988, *J. Chem. Phys.*, 88, 4598
- Jamieson, C. S., Mebel, A. M., & Kaiser, R. I. 2006, *ApJS*, 163, 184
- Jetzki, M., Luckhaus, D., & Signorell, R. 2004, *Canadian J. Chem.*, 82, 915
- Jiang, G. J., Person, W. B., & Brown, K. G. 1975, *J. Chem. Phys.*, 62, 1201
- Johnson, R. E. 1990, *Energetic Charged-Particle Interactions with Atmospheres and Surfaces* (Berlin: Springer)
- Jones, A. P. 2005, in *Proc. The Dusty and Molecular Universe*, ed. A. Wilson (ESA SP-577) (Noordwijk: ESA), 239
- Kaiser, R. I. 2002, *Chem. Rev.*, 102, 1309
- Kaiser, R. I., Eich, G., Gabrysch, A., & Roessler, K. 1997, *ApJ*, 484, 487
- Kerkhof, O., Schutte, W. A., & Ehrenfreund, P. 1999, *A&A*, 346, 990
- Krishnamurthy, R., Arrhenius, G., & Eschenmoser, A. 1999, *Origins Life Evol. Biosphere*, 29, 333
- Kurtz, S. 2006, in *IAU Symp. 231, Astrochemistry: Recent Successes and Current Challenges*, ed. D. C. Lis, G. A. Blake, & E. Herbst (Cambridge: Cambridge Univ. Press), 47
- Leitch-Devlin, M. A., & Williams, D. A. 1984, *MNRAS*, 210, 577
- Linz, H., Stecklum, B., Henning, T., Hofner, P., & Branl, B. 2005, *A&A*, 429, 903
- Liu, S.-Y., Mehringer, D. M., & Snyder, L. E. 2001, *ApJ*, 552, 654
- Macdonald, G. H., Gibb, A. G., Habing, R. J., & Millar, T. J. 1996, *A&AS*, 119, 333
- Mehring, D. M., Snyder, L. E., Miao, Y., & Lovas, F. J. 1997, *ApJ*, 480, L71
- Milligan, D. E., & Jacox, M. E. 1967, *J. Chem. Phys.*, 47, 5146
- . 1971, *J. Chem. Phys.*, 54, 927
- Mohaček-Grošev, V. 2005, *Spectrochim. Acta A*, 61, 477
- Müller, R. P., Hollenstein, H., & Huber, J. R. 1983, *J. Mol. Spectrosc.*, 100, 95
- Nelander, B. 1980, *J. Chem. Phys.*, 73, 1034
- Nummelin, A., Bergman, P., Hjalmarsen, Å., Friberg, P., Irvine, W. M., Millar, T. J., Ohishi, M., & Saito, S. 2000, *ApJS*, 128, 213 (erratum 132, 127 [2001])
- Palumbo, M. E., Castorina, A. C., & Strazzulla, G. 1999, *A&A*, 342, 551
- Prasad, S. S., & Tarafdar, S. P. 1983, *ApJ*, 267, 603
- Remijan, A., Shiao, Y.-S., Friedel, D. N., Meier, D. S., & Snyder, L. E. 2004, *ApJ*, 617, 384
- Remijan, A., Snyder, L. E., Friedel, D. N., Liu, S.-Y., & Shah, R. Y. 2003, *ApJ*, 590, 314
- Remijan, A., Snyder, L. E., Liu, S.-Y., Mehringer, D., & Kuan, Y.-J. 2002, *ApJ*, 576, 264
- Remijan, A. J., & Hollis, J. M. 2006, *ApJ*, 640, 842
- Remijan, A. J., Wyrowski, F., Friedel, D. N., Meier, D. S., & Snyder, L. E. 2005, *ApJ*, 626, 233
- Remijan, A. J., et al. 2006, *ApJ*, 643, 567
- Shapiro, R. 1988, *Origins Life*, 18, 71
- Snyder, L. E. 2006, *Proc. Natl. Acad. Sci.*, 103, 12243
- Sorrell, W. H. 2001, *ApJ*, 555, L129
- Spinks, J. W. T., & Woods, R. J. 1990, *An Introduction to Radiation Chemistry* (3rd ed.; Wiley: New York)
- Strazzulla, G., & Johnson, R. E. 1991, in *Comets in the Post-Halley Era*, ed. R. L. Newburn, Jr., M. Neugebauer, & J. Rahe (Dordrecht: Kluwer), 243
- Talbi, D., Chandler, G. S., & Rohl, A. L. 2006, *Chem. Phys.*, 320, 214
- Tauer, K. J., & Lipscomb, W. N. 1952, *Acta Crystallogr.*, 5, 606
- Tornow, C., Kührt, E., & Motschmann, U. 2005, *Astrobiology*, 5, 632
- Weber, A. L. 1998, *Origins Life*, 28, 259
- Włodarczak, G., & Demaison, J. 1988, *A&A*, 192, 313
- Wooten, A., Włodarczak, G., Mangum, J. G., Combes, F., Encrenaz, P. J., & Gerin, M. 1992, *A&A*, 257, 740